Bayesian location of the QCD critical point: a holographic perspective

Claudia Ratti

UNIVERSITY of HOUSTON

With: M. Hippert, J. Grefa, I. Portillo, J. Noronha, J. Noronha- Hostler, R. Rougemont and M. Trujillo

Motivation

- Is there a critical point on the QCD phase diagram?
- What are the degrees of freedom in the vicinity of the phase transition?
- Where is the transition line at high density?
- What are the phases of QCD at high density?
- What is the nature of matter in the core of neutron stars?

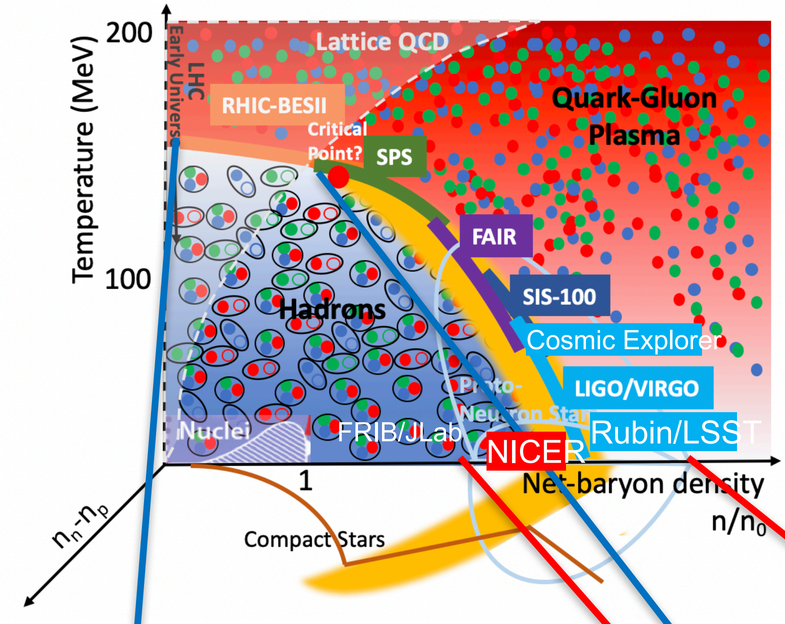

- Run 2019:
  - Collider: $\sqrt{s_{NN}}$=14.6, 19.6, 200 GeV
  - Fixed target: $\sqrt{s_{NN}}$=3.2 GeV
- Run 2020:
  - Collider: $\sqrt{s_{NN}}$=9.2, 11.5 GeV
  - Fixed target: $\sqrt{s_{NN}}$=3.5, 3.9, 4.5, 5.2, 6.2, 7.2, 7.7 GeV
- Run 2021:
  - Collider: $\sqrt{s_{NN}}$=7.7, 17.3 GeV
  - Fixed target: $\sqrt{s_{NN}}$=3.0, 9.2, 11.5, 13.7 GeV

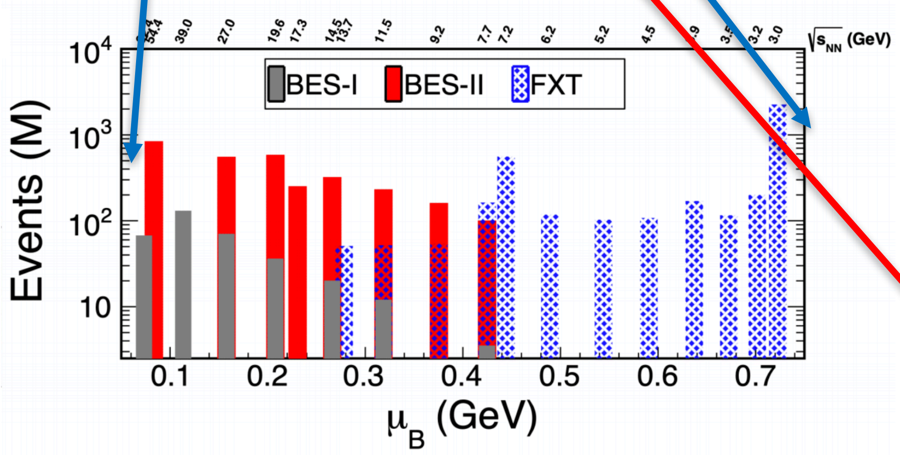

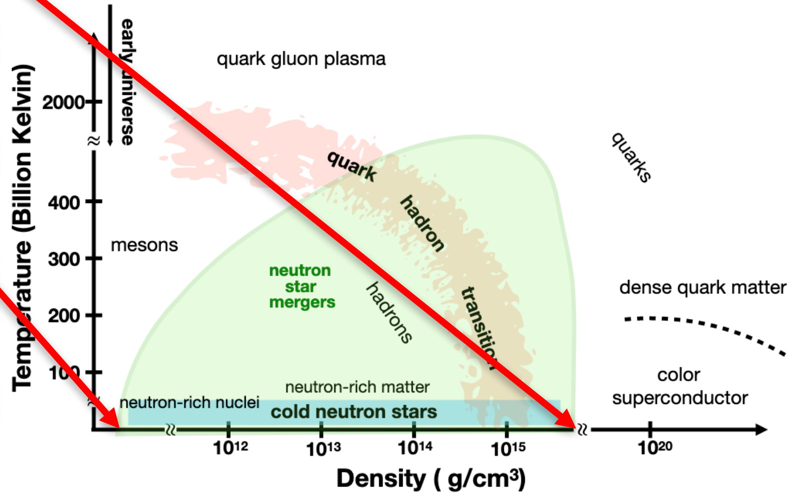

We need models at high μ_B

- Lattice QCD: Equation of state up to $\mu_B/T\sim3.5$

S. Borsanyi et al., PRL (2021)

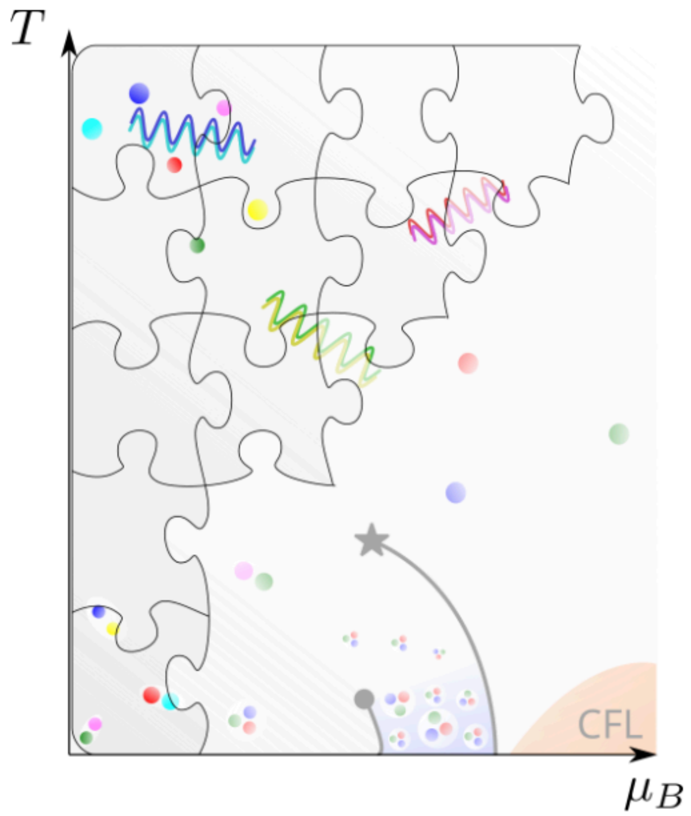

We need models at high μ_B

- Lattice QCD: Equation of state up to $\mu_B/T \sim 3.5$

S. Borsanyi et al., PRL (2021)

- No sign of criticality observed within this region

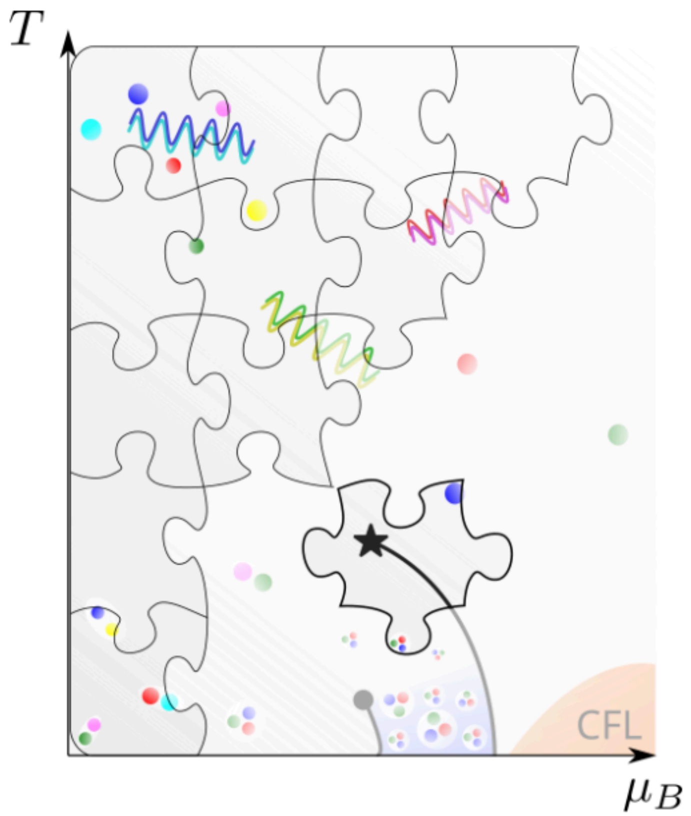

We need models at high μ_B

- Lattice QCD: Equation of state up to $\mu_B/T\sim3.5$

  S. Borsanyi et al., PRL (2021)

- No sign of criticality observed within this region

- Extrapolation: good description of the QGP required

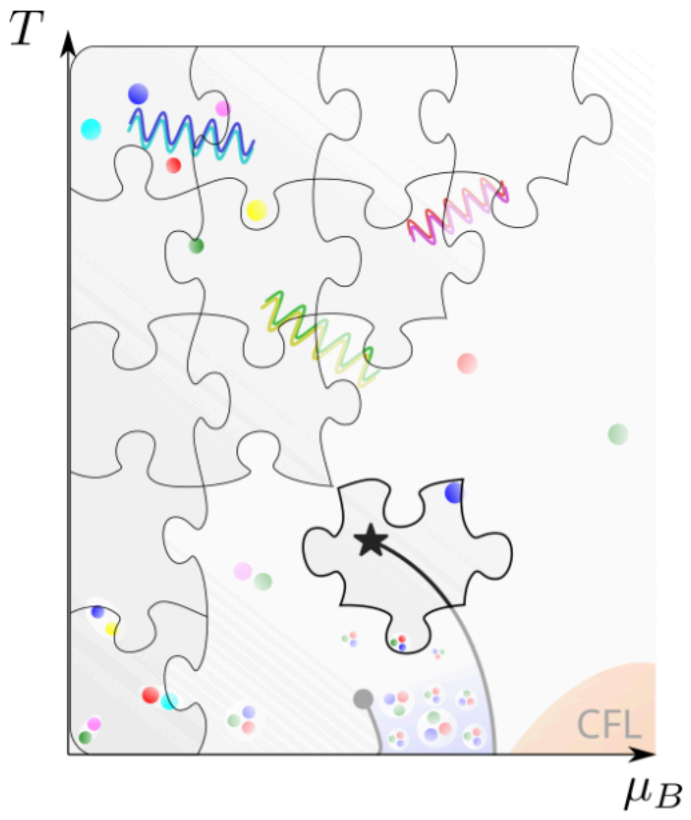

We need models at high μ_B

- Lattice QCD: Equation of state up to $\mu_B/T\sim3.5$

  S. Borsanyi et al., PRL (2021)

- No sign of criticality observed within this region

- Extrapolation: good description of the QGP required

- "Black hole engineering": tweak holographic model to reproduce lattice QCD results

  S. S. Gubser and A. Nellore, PRD (2008)
  O. DeWolfe, S. S. Gubser and C. Rosen, PRD (2011)
  R. Critelli, J. Noronha, J. Noronha-Hostler, I. Portillo,C. R., R. Rougemont, PRD (2017)
  J. Grefa, J. Noronha, J. Noronha-Hostler, I. Portillo,C. R., R. Rougemont, PRD (2021)

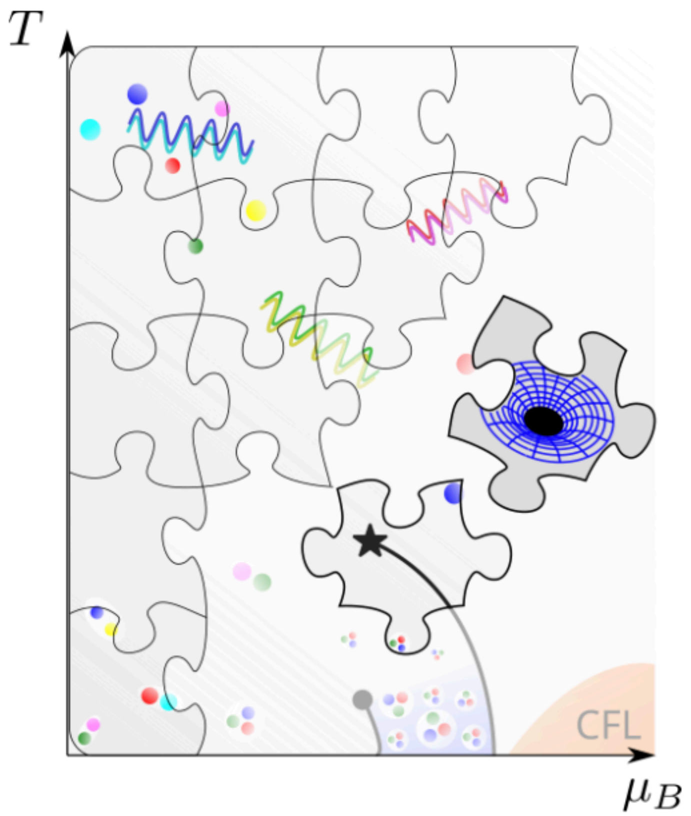

- 5D bulk: Classical gravity with asymptotically Anti-deSitter (AdS5) geometry.
- 3+1D Boundary: Strongly coupled fluid in Minkowski spacetime.

J. M. Maldacena, Adv. Theor. Math. Phys. (1998)

- Black hole: non-zero Hawking temperature and charge
- Strongly coupled, nearly inviscid behavior of the QGP.

P. Kovtun, D. T. Son, A. O. Starinets, PRL (2005)

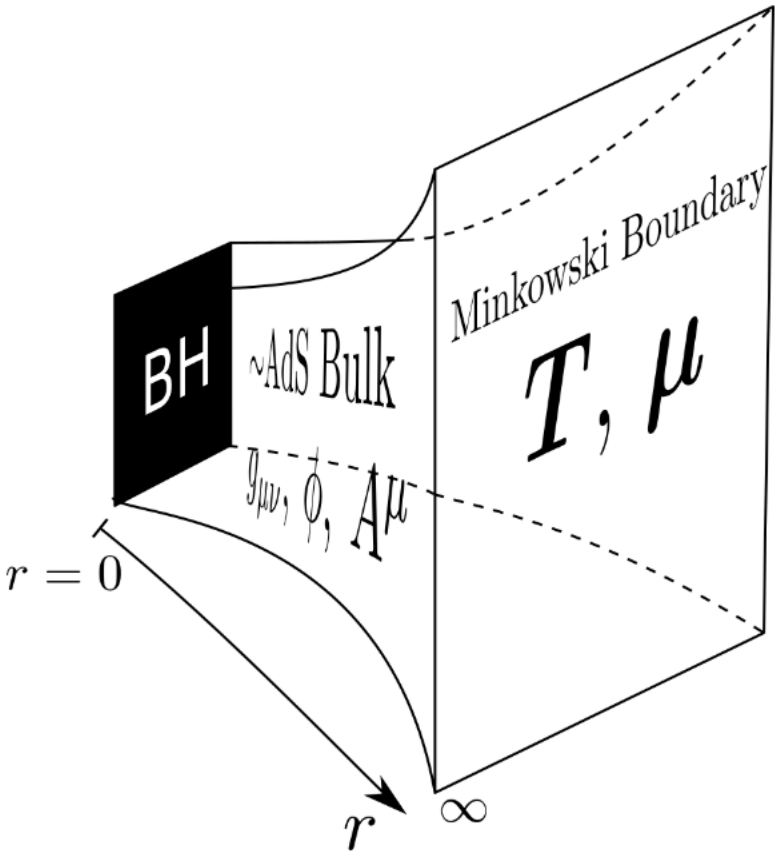

Einstein-Maxwell-Dilaton model

S. S. Gubser and A. Nellore, PRD (2008)
O. DeWolfe, S. S. Gubser and C. Rosen, PRD (2011)
R. Critelli, J. Noronha, J. Noronha-Hostler, I. Portillo, C.R., R. Rougemont, PRD (2017)
J. Grefa, J. Noronha, J. Noronha-Hostler, I. Portillo, C. R., R. Rougemont, PRD (2021)
R. Rougemont et al., Prog. Part. Nucl. Phys. (2024)

- Breaking of conformal symmetry: dilaton field ϕ
- Dual to baryon chemical potential μ: Abelian gauge field A^μ
- Action:

$$S = \frac{1}{2\kappa_5^2} \int_{\mathcal{M}_5} d^5x \sqrt{-g} \left[R - \frac{(\partial_\mu \phi)^2}{2} - V(\phi) - \frac{f(\phi) F_{\mu\nu}^2}{4} \right]$$

- Two potentials: $V(\phi)$ and $f(\phi)$, tweaked to fit lattice QCD results

Einstein-Maxwell-Dilaton model

S. S. Gubser and A. Nellore, PRD (2008)
O. DeWolfe, S. S. Gubser and C. Rosen, PRD (2011)
R. Critelli, J. Noronha, J. Noronha-Hostler, I. Portillo, C.R., R. Rougemont, PRD (2017)
J. Grefa, J. Noronha, J. Noronha-Hostler, I. Portillo, C. R., R. Rougemont, PRD (2021)
R. Rougemont et al., Prog. Part. Nucl. Phys. (2024)

- Breaking of conformal symmetry: dilaton field ϕ.
- Dual to baryon chemical potential μ: Abelian gauge field A^{μ}.
- Action:

$$S = \frac{1}{2\kappa_5^2}\int_{\mathcal{M}_5} d^5x\sqrt{-g}\left[R - \frac{(\partial_\mu\phi)^2}{2} - V(\phi) - \frac{f(\phi)F_{\mu\nu}^2}{4}\right]$$

- Two potentials: $V(\phi)$ and $f(\phi)$, tweaked to fit lattice QCD results

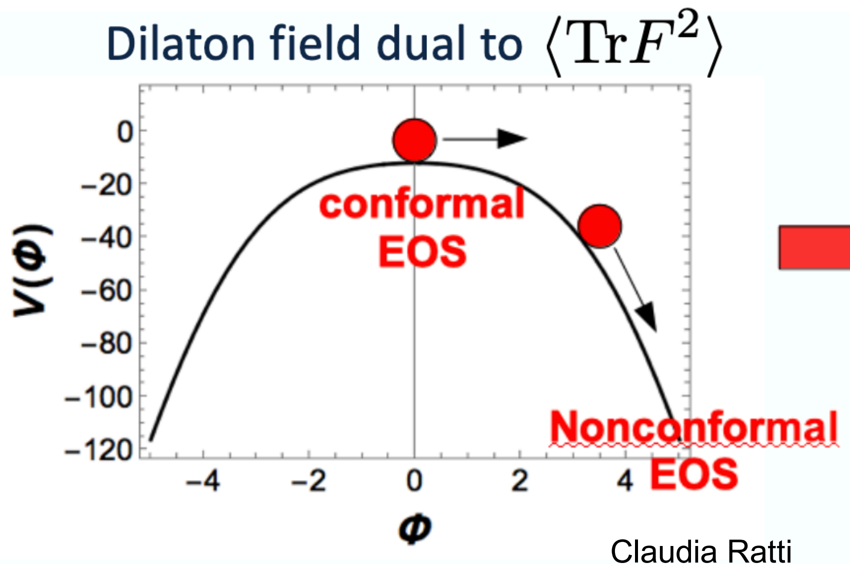

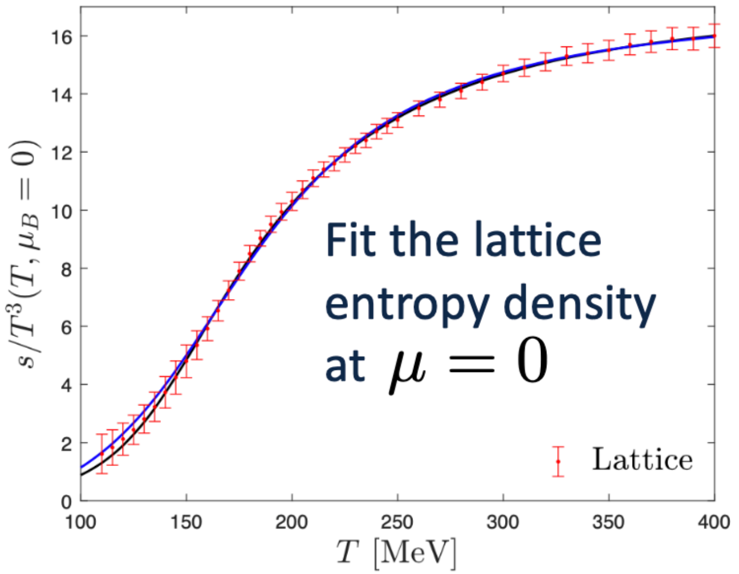

Einstein-Maxwell-Dilaton model

S. S. Gubser and A. Nellore, PRD (2008)
O. DeWolfe, S. S. Gubser and C. Rosen, PRD (2011)
R. Critelli, J. Noronha, J. Noronha-Hostler, I. Portillo, C.R., R. Rougemont, PRD (2017)
J. Grefa, J. Noronha, J. Noronha-Hostler, I. Portillo, C. R., R. Rougemont, PRD (2021)
R. Rougemont et al., Prog. Part. Nucl. Phys. (2024)

- Breaking of conformal symmetry: dilaton field ϕ
- Dual to baryon chemical potential μ: Abelian gauge field A^{μ}
- Action:

$$S = \frac{1}{2\kappa_5^2}\int_{\mathcal{M}_5} d^5x\sqrt{-g}\left[R - \frac{(\partial_\mu\phi)^2}{2} - V(\phi) - \frac{f(\phi)F_{\mu\nu}^2}{4}\right]$$

- Two potentials: $V(\phi)$ and $f(\phi)$, tweaked to fit lattice QCD results

5d gauge field	Conserved baryon charge	Dilaton-Maxwell coupling
$A_\mu \Longrightarrow$	$U(1)_B$	$f(\phi)$

Lattice QCD results: R. Bellwied, C. R. et al., PRD (2015)
S. Borsanyi, C. R. et al., PRL (2021)

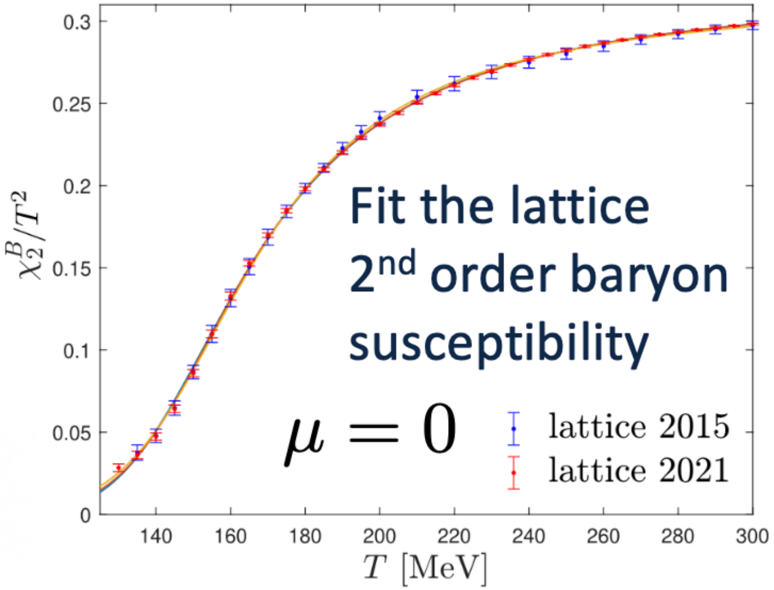

Finite-density properties

muses

- Model predictions agree with lattice QCD results where avaiable

J. Grefa, C. R. et al, Phys. Rev. D (2021)
Lattice results: S. Borsanyi, C. R. et al., PRL (2021)

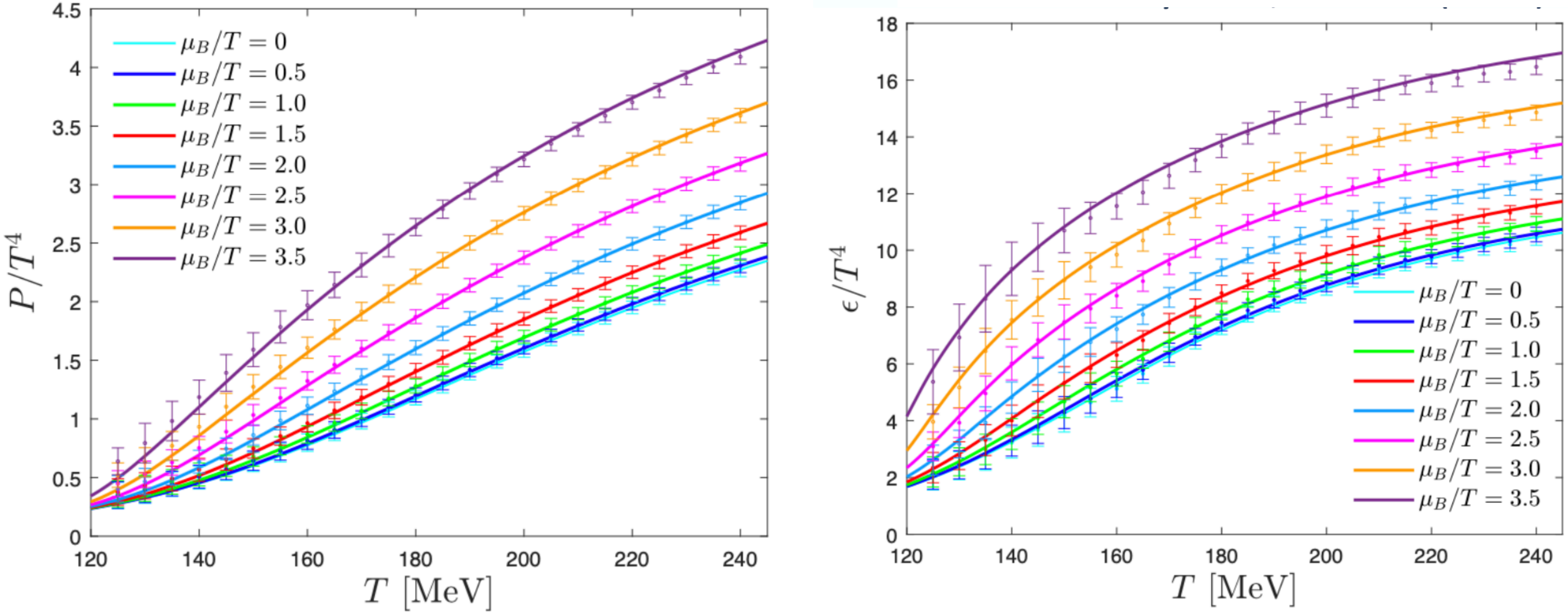

- Powerful, flexible model capable of describing crossover region and beyond

- Real-time calculations also possible

Finite-density properties

muses

- Model predictions agree with lattice QCD results where avaiable

J... a, C. R. et al, Phys. Rev. D (2021)
...esults: S. Borsanyi, C. R. et al., PRL (2021)

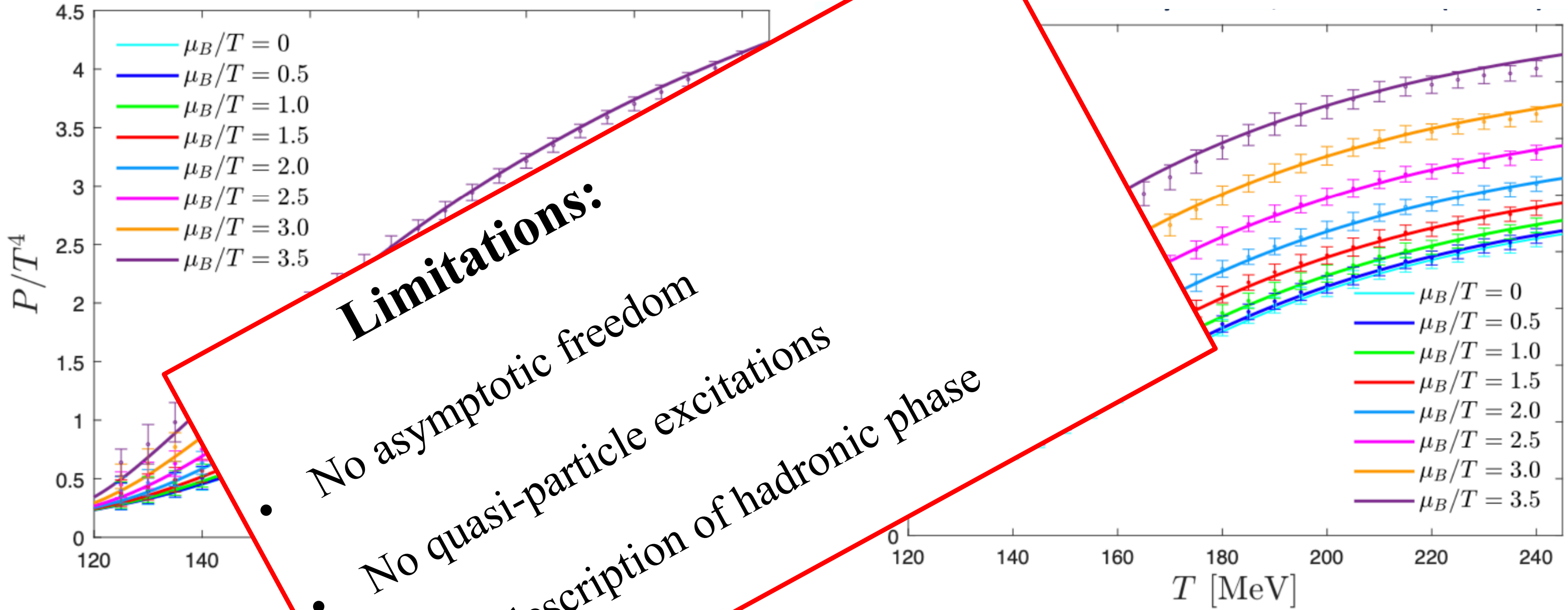

Limitations:

- No asymptotic freedom
- No quasi-particle excitations
- Poor description of hadronic phase

- Powerful, flexible model c... ...ribing crossover region and beyond
- Real-time calculations also possible

Phase diagram from holography

muses

- Dilaton and electric fields at horizon: ϕ_0 and Φ_1 fully specify the physical state
- Lines of constant ϕ_0 can cross.
- Metastable states, spinodal lines
- Critical point: where crossing starts

Fast algorithm to find the critical point!

- Maxwell construction: first order line

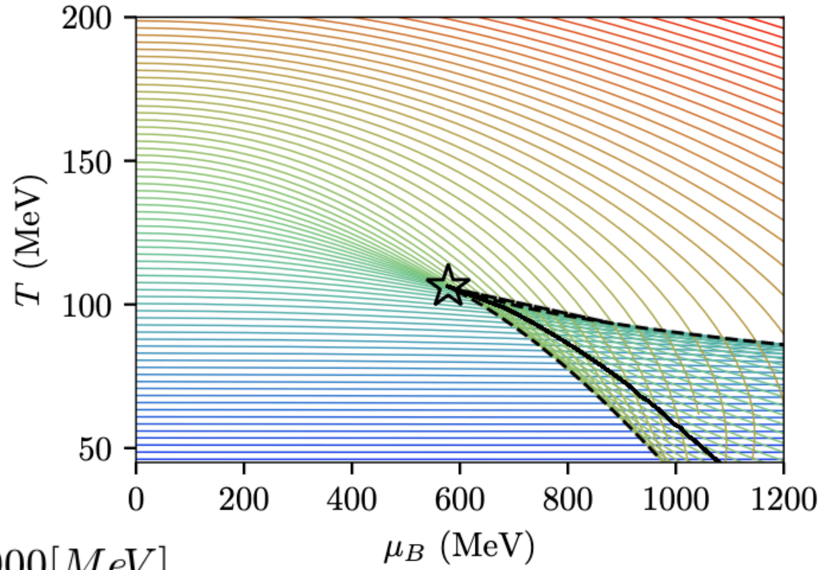

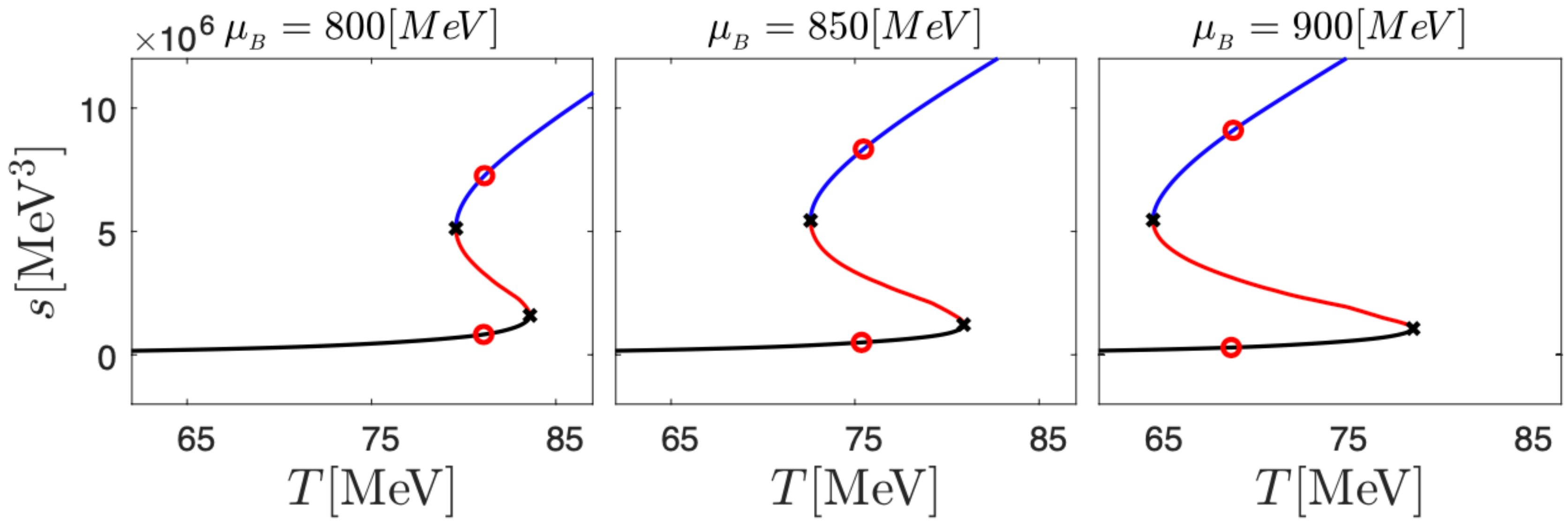

Polynomial-Hyperbolic Ansatz (PHA)

- Interpolates between R. Critelli, C.R. et al., PRD (2017) and R.-G. Cai et al., PRD (2022)

$$V(\phi) = -12\cosh(\gamma\,\phi) + b_2\,\phi^2 + b_4\,\phi^4 + b_6\,\phi^6$$

$$f(\phi) = \frac{\operatorname{sech}(c_1\phi + c_2\phi^2 + c_3\phi^3)}{1+d_1} + \frac{d_1}{1+d_1}\operatorname{sech}(d_2\phi)$$

Parametric Ansatz (PA)

- Similar shapes, more interpretable parameters

$$V(\phi) = -12\cosh\left[\left(\frac{\gamma_1\,\Delta\phi_V^2 + \gamma_2\,\phi^2}{\Delta\phi_V^2 + \phi^2}\right)\phi\right]$$

$$f(\phi) = 1 - (1 - A_1)\left[\frac{1}{2} + \frac{1}{2}\tanh\left(\frac{\phi - \phi_1}{\delta\phi_1}\right)\right] - A_1\left[\frac{1}{2} + \frac{1}{2}\tanh\left(\frac{\phi - \phi_2}{\delta\phi_2}\right)\right]$$

Bayesian black-hole engineering

muses

- What scenarios described by model compatible with the lattice results + error bars?
- Systematic scan over possible extrapolations to higher densities.
- Use Bayesian inference tools.

Bayes' Theorem

$$\underbrace{P\left(\text{model}\,\middle|\,\text{results}\right)}_{\text{posterior } \mathcal{P}} \times P\left(\text{results}\right) = \underbrace{P\left(\text{results}\,\middle|\,\text{model}\right)}_{\text{likelihood } \mathcal{L}} \times \underbrace{P\left(\text{model}\right)}_{\text{prior knowledge}}$$

Gaussian Likelihood

$$\mathcal{L} = \exp\left\{-\frac{1}{2}\boldsymbol{\delta x}^T\boldsymbol{\Sigma}^{-1}\boldsymbol{\delta x} - \frac{1}{2}\log\det\boldsymbol{\Sigma} + \text{constant}\right\}$$

- $\boldsymbol{\delta x}$: deviation for $s(T)$ and $\chi_2^{(B)}(T)$ at $\mu = 0$.
- Correlation $\Gamma \equiv \exp\left(-\Delta T/\xi_T\right)$ between neighboring points $\rightarrow$ extra model parameter.

Markov Chain Monte Carlo (MCMC)

muses

- Random evolution to sample from posterior
- Transition probabilities such that $\mathcal{P}$ is stationary limit
- Differential evolution MCMC: suited for correlations

C.J.F. Ter Braak, Statistics and Computing 16 (2006)

Differential evolution

1. Use other chains j, k to update chain $i \neq j \neq k$: $\theta_i \to \theta_i + \frac{b}{\sqrt{2d}}(\theta_j - \theta_k) + \xi_i$.
2. Compute $\mathcal{P}$ from model EoS.
   - If $\mathcal{P}/\mathcal{P}_0 > 1$, transition to new parameters.
   - Otherwise, accept transition with probability $\mathcal{P}/\mathcal{P}_0$.
3. Repeat.

- **Inputs:** baryon susceptibility and entropy density from lattice QCD

Results

- Flat prior for parameters
- 20% of prior samples give no critical point

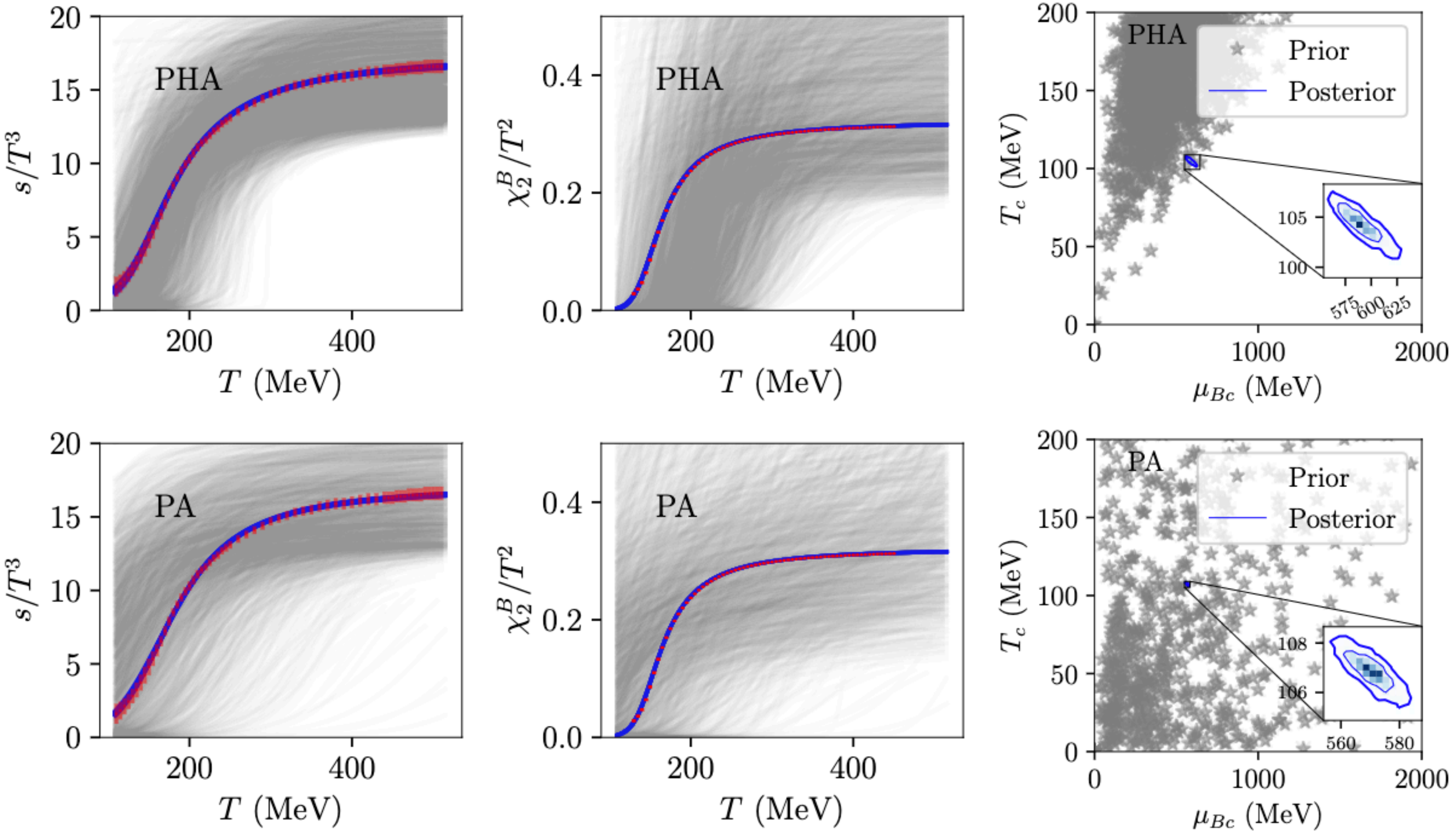

M. Hippert, C. R. et al, arXiv:2309.00579.

Posterior critical points

- All posterior predictions for the critical point location collapse around these regions

$$(T_c,\, \mu_{Bc})_{PHA} = (104 \pm 3,\, 589^{+36}_{-26})\ \text{MeV}, \qquad (T_c,\, \mu_{Bc})_{PA} = (107 \pm 1,\, 571 \pm 11)\ \text{MeV}$$

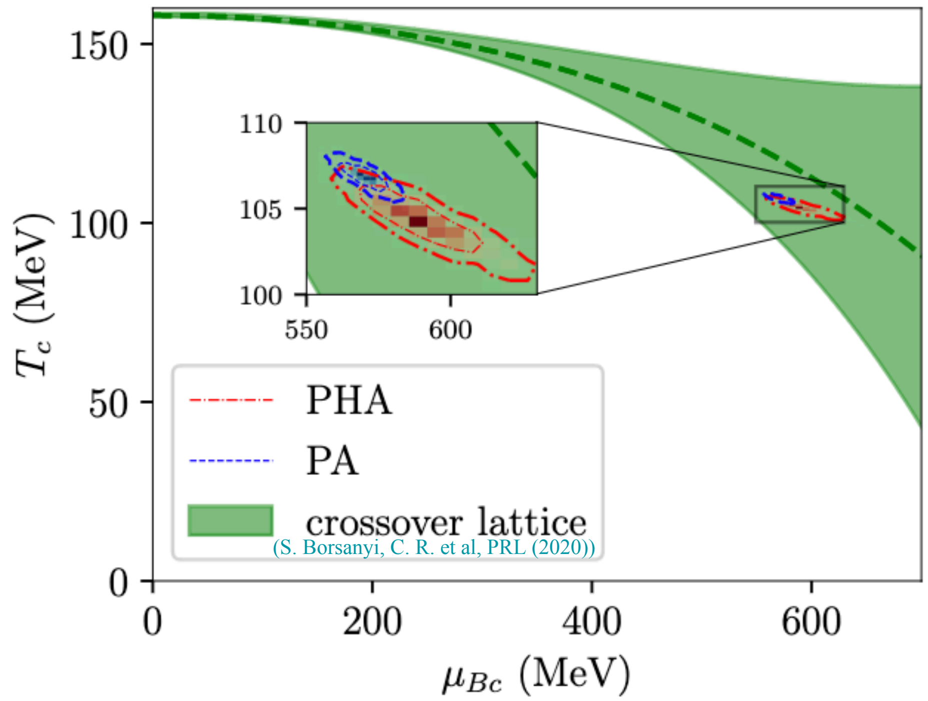

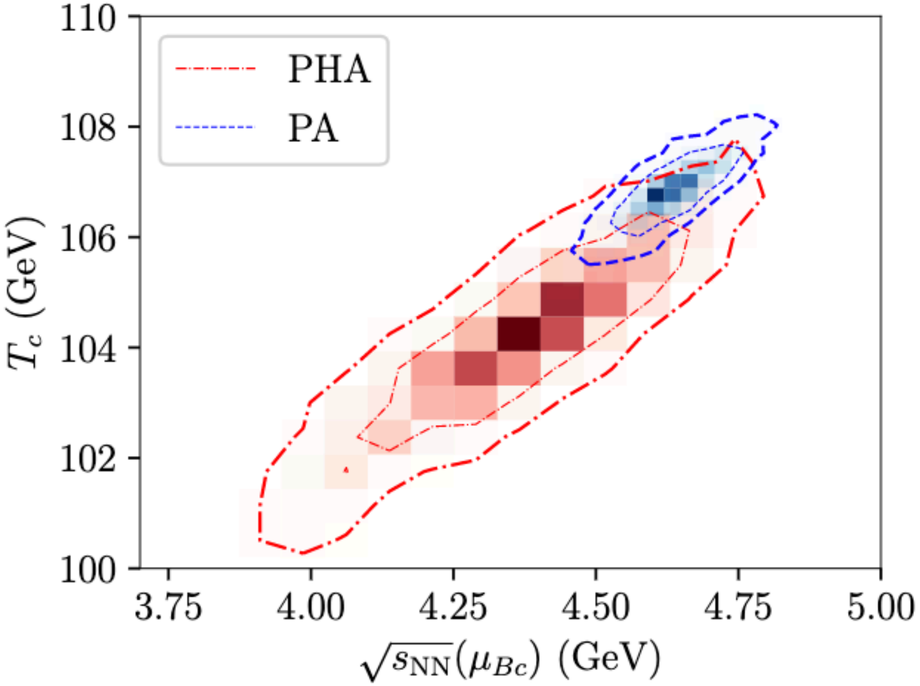

Both Ansätze overlap at $1\,\sigma$. **Robust results!**

M. Hippert, C. R. et al, arXiv:2309.00579.

Similar locations are found in FRG, DSE and Pade estimates

Gunkel, Fischer, PRD (2021)
Fu, Pawlowski, Rennecke, PRD (2020)
G. Basar, PRL (2021)
P. Dimopoulos et al., PRD (2022)

Posterior critical points

- All posterior predictions for the critical point location collapse around these regions

$$(T_c,\ \mu_{Bc})_{PHA} = (104 \pm 3,\ 589^{+36}_{-26})\ \text{MeV}, \qquad (T_c,\ \mu_{Bc})_{PA} = (107 \pm 1,\ 571 \pm 11)\ \text{MeV}$$

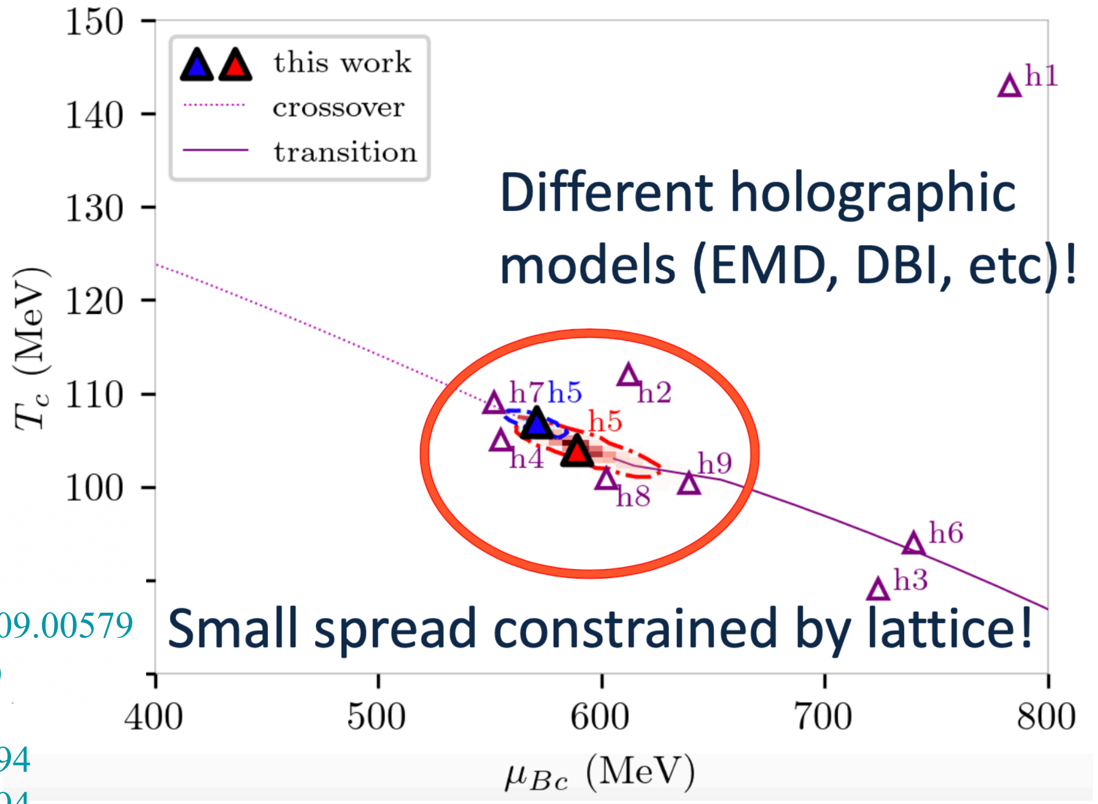

h1: O. DeWolfe et al., PRD (2011)
h2: J. Knaute et al., PLB (2018)
h3: R. Critelli et al., PRD (2017)
h4: R.-G. Cai, PRD (2022)
h5: M. Hippert, C. R. et al, arXiv:2309.00579
h6: X. Chen, M. Huang, PRD (2024)
h7: Q. Fu et al., arXiv:2404.12109
h8: N. Jokela et al., arXiv: 2405.02394
h9: N. Jokela et al., arXiv: 2405.02394

Similar locations are found in FRG, DSE and Pade estimates

Gunkel, Fischer, PRD (2021)
Fu, Pawlowski, Rennecke, PRD (2020)
G. Basar, PRL (2021)
P. Dimopoulos et al., PRD (2022)

Conclusions

- Powerful description of the QGP, matching finite-density lattice QCD results

- Larger statistical preference for a critical point after constraints: PA model: ~80% of prior → 100% of posterior

- All posterior predictions for the critical point location collapse around these regions

$$(T_c,\, \mu_{Bc})_{PHA} = (104 \pm 3,\, 589^{+36}_{-26})\ \text{MeV}, \qquad (T_c,\, \mu_{Bc})_{PA} = (107 \pm 1,\, 571 \pm 11)\ \text{MeV}$$

- Other approaches (FRG, DSE, Pade) find very similar results

Backup slides

New C++ code

muses

- Development within the MUSES Framework: Multi-institutional collaboration for a unified solver for the equation of state, bridging models and applications

- Support and advising by cyberinfrastructure and computer-science experts T. Andrew Manning and Roland Haas

- Improved method to extract asymptotic UV scaling and thermodynamics

- Large boost in performance and numerical stability

muses

Correlation strength

- The parameter Γ is an indicator for the correlation among lattice data between neighboring points

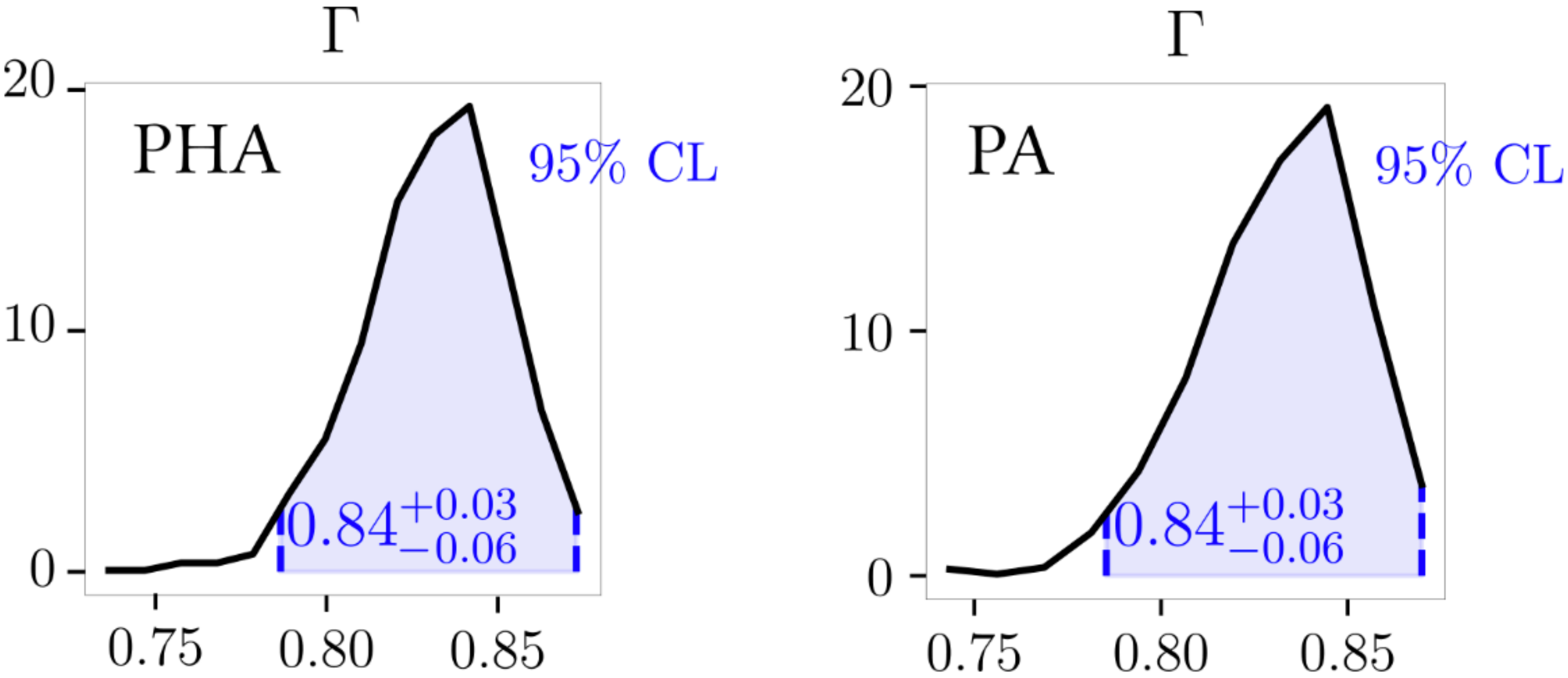

Equations of motion

muses

$$\phi''(r) + \left[\frac{h'(r)}{h(r)} + 4A'(r) - B'(r)\right]\phi'(r) - \frac{e^{2B(r)}}{h(r)}\left[\frac{\partial V(\phi)}{\partial \phi} + \right.$$

$$\left. - \frac{e^{-2[A(r)+B(r)]}\Phi'(r)^2}{2}\frac{\partial f(\phi)}{\partial \phi}\right] = 0,$$

$$\Phi''(r) + \left[2A'(r) - B'(r) + \frac{d[\ln f(\phi)]}{d\phi}\phi'(r)\right]\Phi'(r) = 0,$$

$$A''(r) - A'(r)B'(r) + \frac{\phi'(r)^2}{6} = 0,$$

$$h''(r) + [4A'(r) - B'(r)]h'(r) - e^{-2A(r)}f(\phi)\Phi'(r)^2 = 0,$$

$$h(r)[24A'(r)^2 - \phi'(r)^2] + 6A'(r)h'(r) +$$
$$+2e^{2B(r)}V(\phi) + e^{-2A(r)}f(\phi)\Phi'(r)^2 = 0,$$

Extraction of thermodynamics

muses

- Thermodynamics extracted from scalings after conversion to physical units.
- Requires near-boundary scalings,

$$\phi \sim \phi_A \, e^{-\nu A(r)}, \quad \Phi \sim \Phi_0^{\text{far}} + \Phi_2^{\text{far}} \, e^{-2A(r)}, \quad A \sim A_{-1}^{\text{far}} \, r + A_0^{\text{far}}$$

- Inversion to find ϕ_A and Φ_2^{far}:

  large coefficient $\times$ tiny number $=$ pure noise.

PHA model

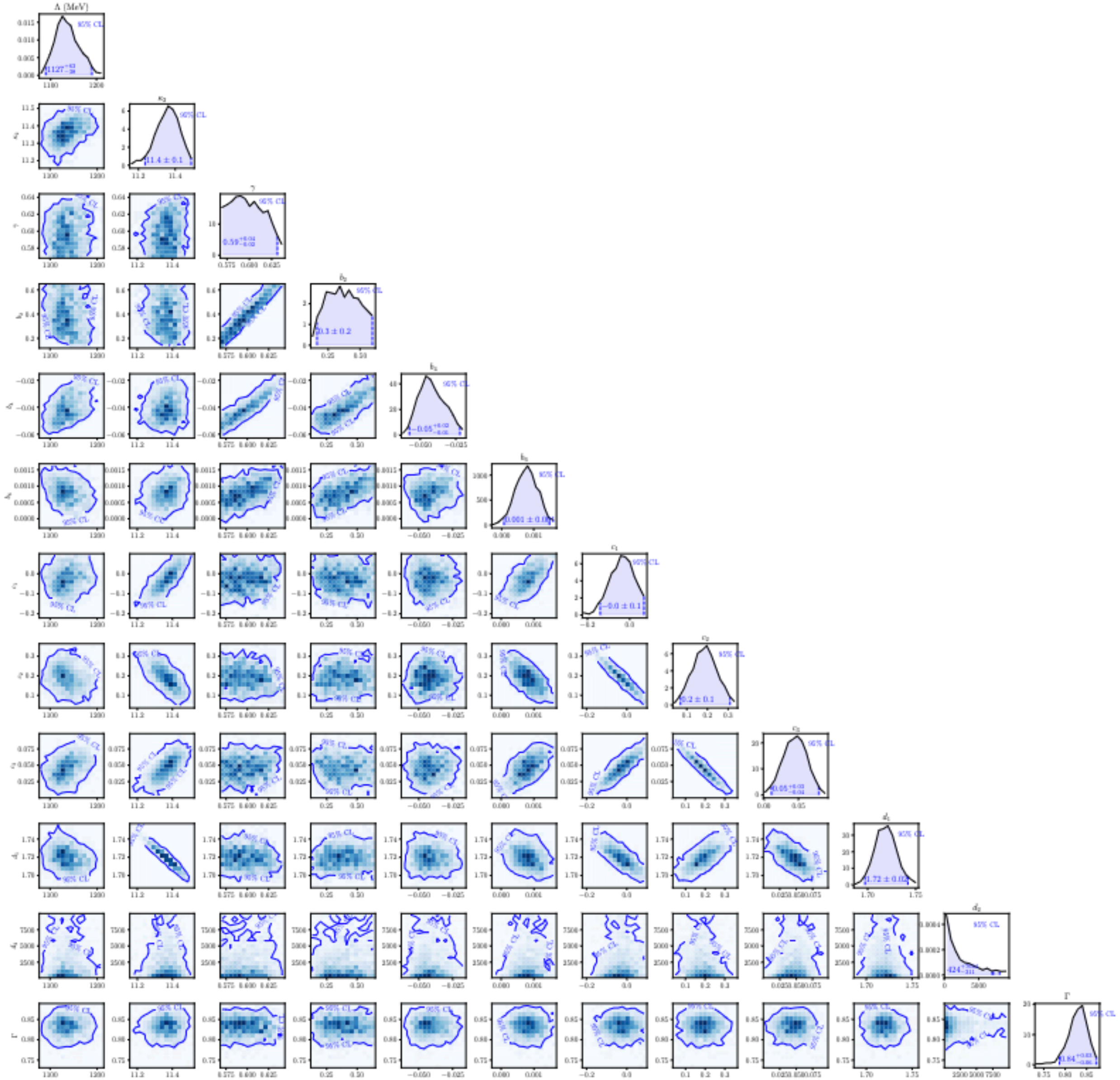
Λ (MeV)
95% CL
95% CL
95% CL
95% CL
95% CL
95% CL
95% CL
95% CL
95% CL
95% CL
95% CL
95% CL

PA model

muses

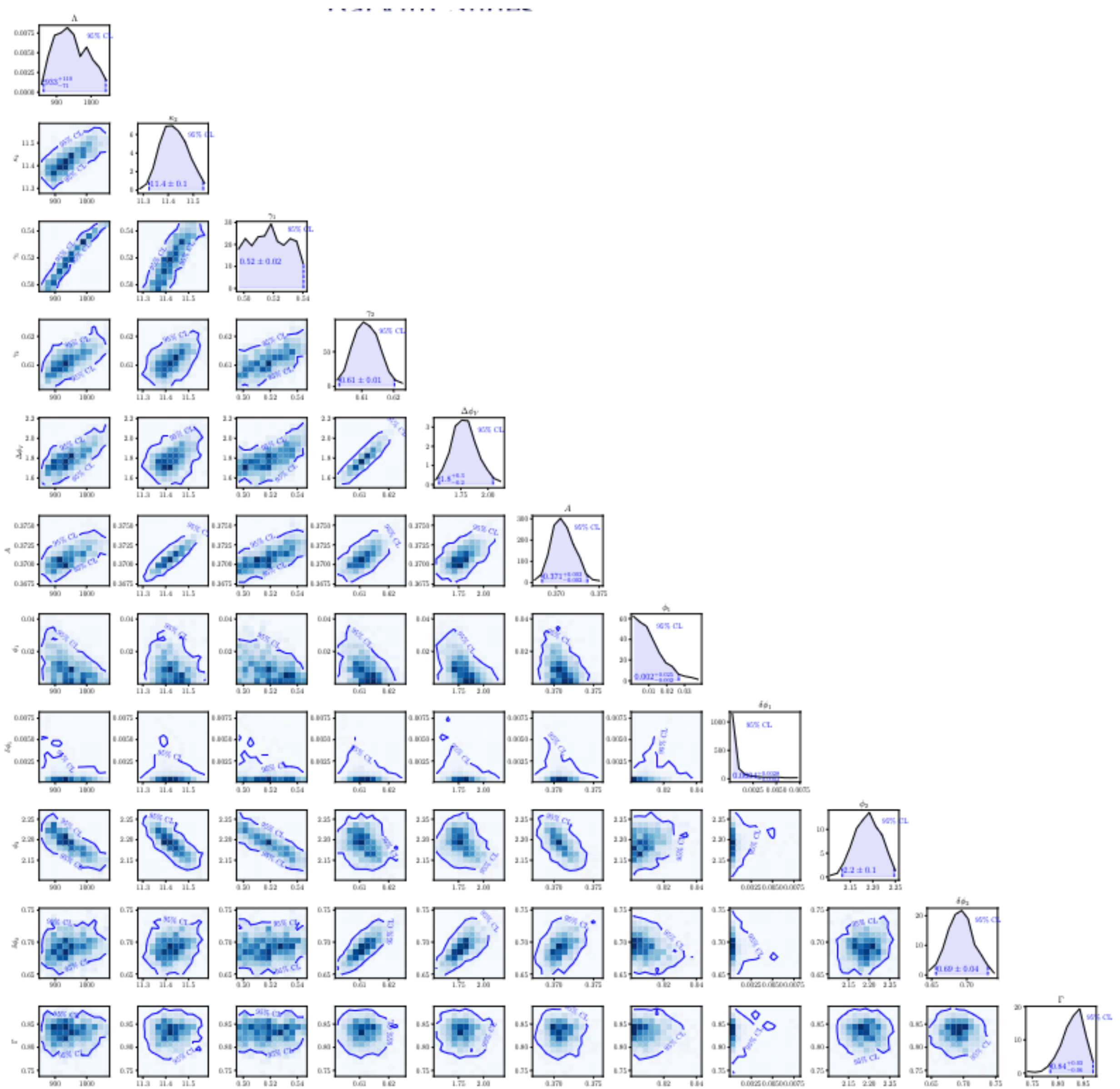

PHA Potentials

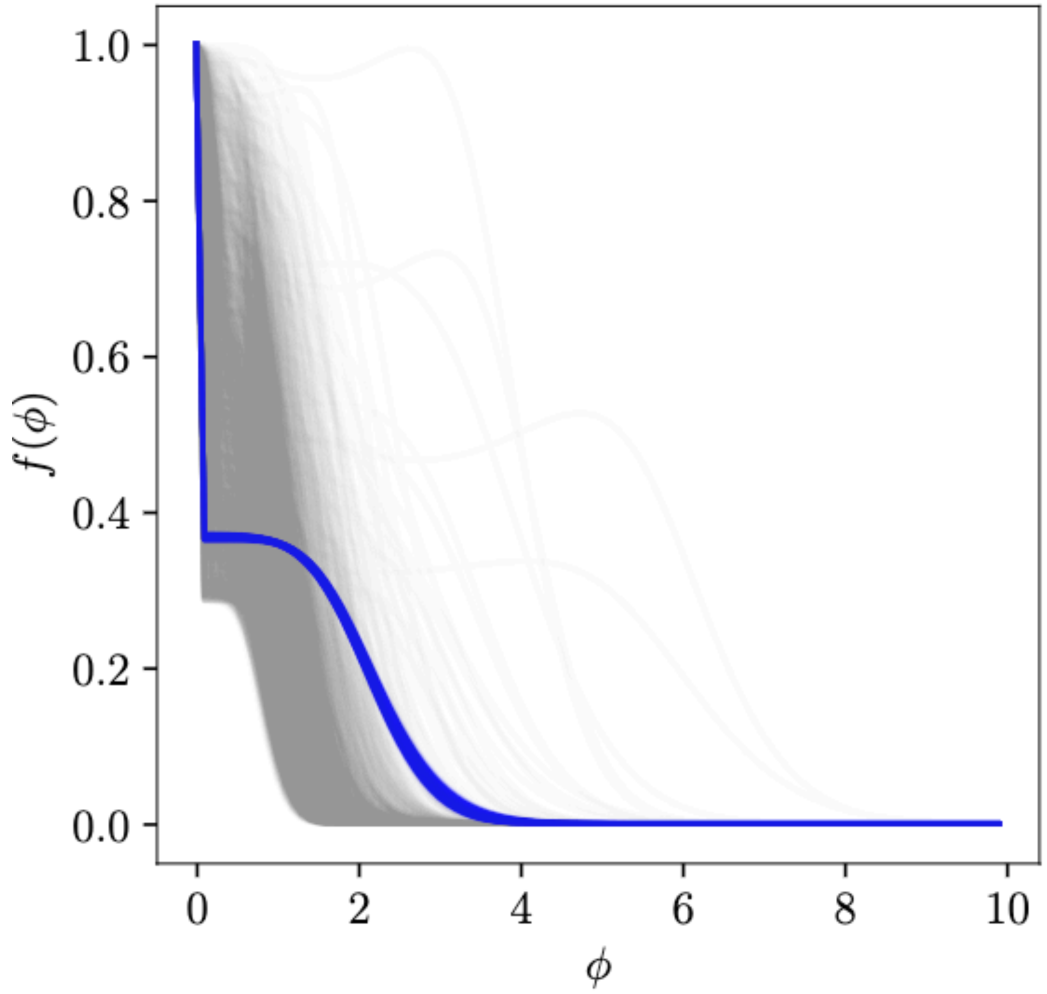

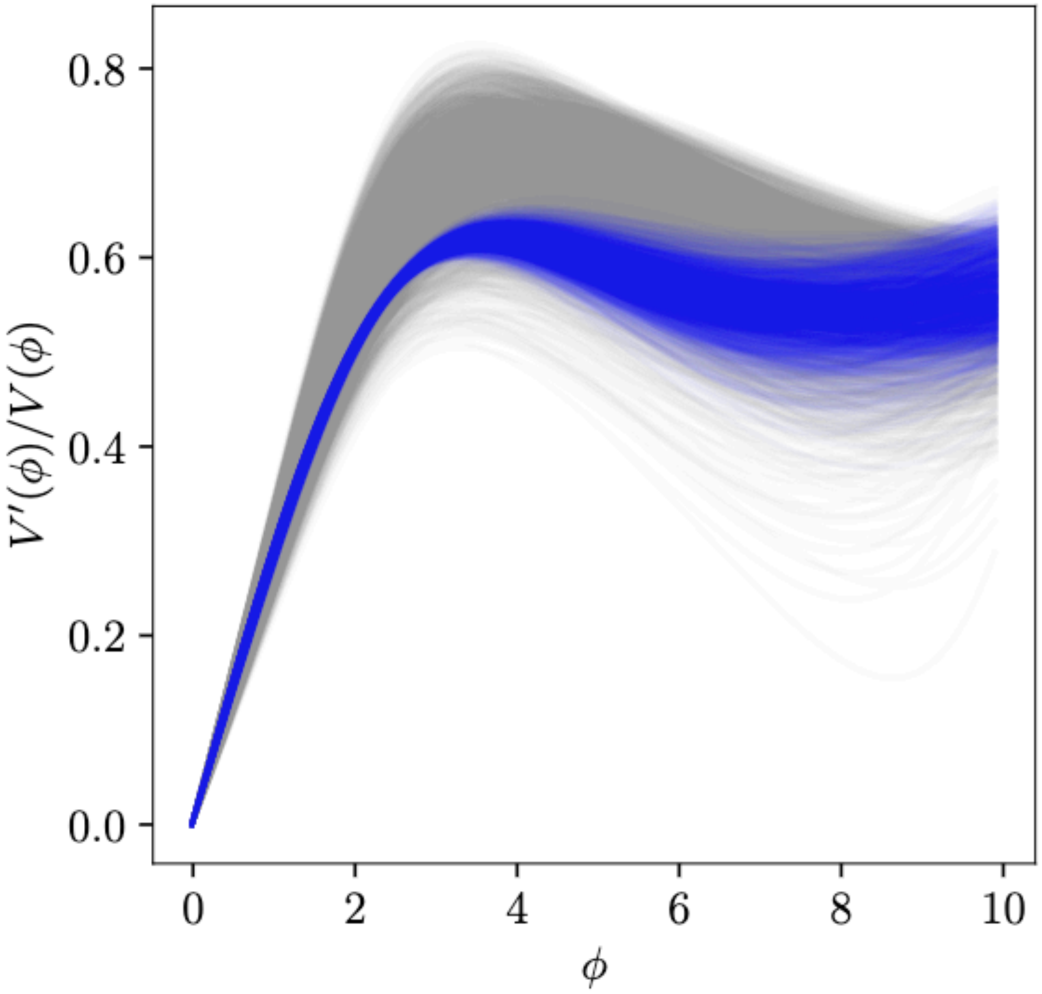

PA Potentials